$2n$-transfer contribution in the ^{4}He(^{6}He,^{6}He)^{4}He cross section at $E_{\text{c.m.}}=11.6$ MeV

R. Raabe,* A. Andreyev,† M. Huyse, A. Piechaczek,‡ P. Van Duppen, L. Weissman,§ and A. Wöhr‖
Instituut voor Kern- en Stralingsfysica, University of Leuven, B-3001 Leuven, Belgium

C. Angulo, S. Cherubini,¶ and A. Musumarra**
Centre de Recherches du Cyclotron and Institut de Physique Nucléaire, Université Catholique de Louvain, B-1348 Louvain-la-Neuve, Belgium

D. Baye and P. Descouvemont
Physique Nucléaire Théorique et Physique Mathématique, Case Postale 229, Université Libre de Bruxelles, B-1050 Brussels, Belgium

T. Davinson, A. Di Pietro,** A. M. Laird, A. Ostrowski,†† and A. Shotter‡‡
Department of Physics & Astronomy, University of Edinburgh, Edinburgh EH9 3JZ, United Kingdom

L. I. Galanina and N. S. Zelenskaya
Nuclear Physics Institute, Lomonosov Moscow State University, 119899 Moscow, Russia
(Received 26 November 2002; published 2 April 2003)

The ^{6}He + ^{4}He elastic scattering cross section was measured at $E_{\text{c.m.}}=11.6$ MeV using a ^{6}He radioactive beam and a ^{4}He-implanted Al foil as target. The use of the thin implanted target allowed to enlarge the angular range in which the data were collected, with respect to a previous measurement at the same center-of-mass energy. The new and previous data are compared with several calculations. The inclusion of a description for the $2n$-transfer process, either with a parity-dependent term, or with a distorted-wave Born approximation transfer amplitude, is crucial to reproduce the increase of the cross section at large angles, thus assessing the contribution of the $2n$-transfer process to the reaction. At the present energy, the complicated nature of the transfer process and the possible role played by the coupling to other channels, in particular, the breakup, require sophisticated reaction models in order to extract the relevant information on the peculiar ^{6}He nucleus. The quality of the data is such that the differences between ^{6}He and the similar ^{6}Li system should be identified by such calculations.

DOI: 10.1103/PhysRevC.67.044602 PACS number(s): 25.10.+s, 25.60.Bx, 25.60.Je

I. INTRODUCTION

The discovery of halo phenomena in nuclei is due to a series of experiments by I. Tanihata and his collaborators in the mid-80s [1,2], when a large interaction cross section was measured for the neutron-rich ^{6}He and ^{11}Li isotopes on different targets. Shortly after, those results were explained in a simple and elegant way in Ref. [3], by modeling the ^{11}Li nucleus as a ^{9}Li core plus a neutron pair: the low binding energy of the latter would allow the neutrons to tunnel out from the core, forming a dilute veil of matter (the halo), which would extend into the classically forbidden region. By similarity, the concept of halo was also extended to the ^{6}He system, though the phenomenon is in ^{6}He less remarkable than in ^{11}Li. Further experimental evidence of the peculiar nature of the ^{6}He and ^{11}Li nuclei came from the measurement of narrow momentum distributions of fragments from breakup reactions [4–7], the low-lying E1 strength obtained from electromagnetic dissociation [8,9], and the distribution of the Gamow-Teller strength from β decay [10].

The features of halo nuclei are better reproduced in terms of few cluster models, two- or three-body systems [11–13], rather than using the shell model. The halo in ^{11}Li is more pronounced, due to the very small two-neutron separation energy; all related effects are expected to be enhanced. The ^{6}He nucleus, on the other hand, presents two major advantages: (1) the study of its structure in terms of a three-cluster model can profit from the good knowledge of the α core configuration, and of the α-n and n-n interactions (in contrast, the structure of the ^{9}Li core and the ^{9}Li-n interaction in ^{11}Li are less known); (2) experimentally, beams of ^{6}He ions have been available for the last seven years with a quality and variety in energy not matched by the ^{11}Li beams. The focus of the research on halos has therefore been, in the recent years, on the ^{6}He nucleus.

*Present address: DSM/DAPNIA/SPhN, CEA Saclay, France. Electronic address: raabe@cea.fr
†Present address: University of Liverpool, United Kingdom.
‡Present address: Oak Ridge National Laboratory, Oak Ridge, TN 37831.
§Present address: National Superconducting Cyclotron Laboratory, Michigan State University, East Lansing, MI 48824.
‖Present address: Argonne National Laboratory, Argonne, IL 60439.
¶Present address: Ruhr Universität Bochum, Germany.
**Present address: Istituto Nazionale di Fisica Nucleare, Laboratori Nazionali del Sud, Catania, Italy.
††Present address: Johannes Gutenberg University, Mainz, Germany.
‡‡Present address: TRIUMF, Vancouver, Canada.

A major part of the research is dedicated to understand in which way halo nuclei may influence known reaction processes, in particular, fusion, through their large matter distribution and the strong coupling to the breakup channels due to their weakly bound nature [14–18]. Another research interest is the halo structure itself and the correlation between the neutrons that form the halo. High energy fragmentation reactions have been used for these studies, but the quantities accessible in such measurements proved to be strongly influenced by the reaction mechanism [19,20]. In this respect, transfer reactions of the halo neutrons on simple targets (protons, α particles) [21–24] may provide a better insight on the halo structure. In addition, in most cases the measurement of the transfer cross section involves that of the direct elastic scattering on the same target; this provides the means to obtain the useful parameters of the optical potential, important also to understand the results of the fusion reactions.

On these grounds, we have performed an investigation of the ^{4}He(^{6}He, ^{6}He) ^{4}He elastic scattering at low energy. The two-neutron transfer process, which takes place between two identical α cores (elastic transfer [25]), produces the same two particles in the exit channel, hence it also appears as elastic scattering. Together with other transfer data at similar and higher energy, these results can be compared with the models in order to extract relevant information about the peculiar structure of ^{6}He.

The results presented in this paper are from the last measurement of a campaign, in which the elastic scattering of ^{6}He on different targets (protons, ^{4}He, Al, Pb, and Au targets) was investigated. The first elastic scattering data of ^{6}He on ^{4}He were presented in a previous paper [22]. Those data, collected at $E_{\mathrm{c.m.}}=15.9$ MeV and $E_{\mathrm{c.m.}}=11.6$ MeV, were limited in the angular range between 50° and 140° in the center-of-mass system. The new data, reported here, were collected again at the lower energy, $E_{\mathrm{c.m.}}=11.6$ MeV, but in a much wider angular range.

In Sec. II of this paper we provide some experimental details about the measurement we performed, together with an explanation of the procedure followed to extract the cross-section data. Section III is dedicated to a discussion of the results that are analyzed by using different models and are compared with ^{6}Li+ ^{4}He elastic scattering data at a similar energy. In Sec. IV a summary and the conclusions are presented.

II. EXPERIMENTAL DETAILS

The measurements were performed at the Cyclotron Research Centre in Louvain-la-Neuve, Belgium. The intense ^{6}He beam is produced by the isotope-separation-on-line (ISOL) technique using two coupled cyclotrons, CYCLONE 30 and CYCLONE 110. Details about the production of the ^{6}He beam can be found in Ref. [26]. Briefly, an intense proton beam (200 μA) delivered by CYCLONE 30 impinges on a LiF target, where the ^{6}He nuclei are produced in the ^{7}Li(p,2p)^{6}He reaction. The nuclei diffuse out of the target and are collected and ionized in an electron cyclotron resonance (ECR) ion source. They are then injected and accelerated in CYCLONE 110, which also acts as a mass separator. An upper limit of 10^{-4} could be estimated for possible contaminants (such as ^{6}Li) from the absence of related events in the collected data. The beam intensity at the target position for this measurement was 7.7×10^5 s^{-1} for 60 hours of irradiation (^{6}He in 2^+ charge state, at $E_{\mathrm{lab}}=29.1$ MeV).

In our previous measurements of the ^{4}He(^{6}He, ^{6}He) ^{4}He elastic scattering we used a ^{4}He static gas target [22]. This technique provided a large amount of target nuclei; however, it limited the accessible angular range due to its geometry and the large energy loss of outgoing particles in the window of the gas cell. To overcome this problem, in the present setup we prepared and used a thin ^{4}He-implanted Al foil as target.

The foils, 0.7 μm thick, were implanted at the Leuven isotope separator, using ^{4}He beams of various energies between 20 and 80 keV. The amount of ^{4}He content retained in the foils was then measured by proton Rutherford backscattering spectroscopy RBS at the Tandetron accelerator of the Laboratoire d'Analyses par réactions nucléares (LARN) laboratory of the University of Namur [27]. Further details about the preparation of the implanted targets can be found in [28,29]. The foil with the largest amount of ^{4}He nuclei was used for the ^{4}He(^{6}He, ^{6}He) ^{4}He cross-section measurement at Louvain-la-Neuve. The ^{4}He thickness was 2.7×10^{17} particles/cm^2; impurities due to protons, ^{12}C and ^{16}O were present on the surfaces of the foil in amounts comparable with the number of ^{4}He atoms. The impurities did not disturb the subsequent ^{4}He(^{6}He, ^{6}He) ^{4}He measurement, as a clear selection of the events of interest was possible. The ^{4}He thickness was almost a factor 50 less than that of the gas target previously used. However, the intensity of the ^{6}He radioactive beam had increased due to the possibility of using a higher current for the primary proton beam; this, and a longer irradiation time, allowed to perform the measurement successfully.

The detection setup consisted of 14 segments of the Louvain-la-Neuve-Edinburgh detector array (LEDA) of silicon-strip detectors [30]. Each segment has an aperture of 45° and is divided into 16 annular strips. The detectors were placed in a configuration similar to the one used in the previous measurements and described in Ref. [22]. This setup provided a very good angular coverage in the forward hemisphere, combined with a high segmentation at small laboratory angles. The energy and time of flight (with respect to the cyclotron radio frequency) of all charged particles hitting the detectors were recorded. Determination of the beam dose was performed from the direct beam current measurement on a Faraday cup placed behind the detection setup; the correct normalization of this reading was obtained using a measurement of the elastic scattering of ^{6}He on a thin Au target of known thickness.

The position of the detectors was optimized in order to allow the coincident detection of both outgoing particles from the ^{4}He(^{6}He, ^{6}He) ^{4}He elastic scattering events in a wide angular range, with particular attention to the small and large center-of-mass angles. The coincident detection of the ^{6}He and ^{4}He particles was essential to provide the signature for the events of interest; these were then identified among other multiplicity-two events through the reconstruction of

TABLE I. Cross-section data for the ^{4}He(^{6}He, ^{6}He)^{4}He elastic scattering at $E_{\text{c.m.}}=11.6$ MeV, obtained with the ^{4}He-implanted Al target.

$\theta_{\text{c.m.}}$ (degrees)	$d\sigma/d\Omega$ (mb/sr)	$\delta(d\sigma/d\Omega)$ (mb/sr)	$\theta_{\text{c.m.}}$ (degrees)	$d\sigma/d\Omega$ (mb/sr)	$\delta(d\sigma/d\Omega)$ (mb/sr)
20.8	326.6	91.5	93.5	4.17	0.59
22.0	313.3	49.8	96.5	1.85	0.39
23.2	236.1	35.4	99.5	0.59	0.22
24.4	171.1	23.1	102.5	0.26	0.15
25.7	157.3	15.7	105.5	1.22	0.33
26.9	139.2	9.3	108.5	2.73	0.49
28.1	110.3	7.5	111.5	4.08	0.61
29.3	78.8	5.4	114.5	7.39	0.83
30.6	60.9	4.7	117.5	8.63	0.93
31.8	45.2	4.0	120.5	11.10	1.21
69.5	5.19	2.59	123.5	14.83	2.26
72.5	7.10	1.77	126.5	3.87	2.24
75.5	8.64	1.22	155.3	37.2	$^{+5.3}_{-16.4}$
78.5	9.51	1.00	157.2	49.4	$^{+4.5}_{-31.5}$
81.5	10.54	0.98	159.0	54.6	$^{+5.1}_{-41.4}$
84.5	8.81	0.87	160.8	62.1	$^{+7.7}_{-43.6}$
87.5	8.20	0.83	162.5	150.9	$^{+37.7}_{-111.1}$
90.5	6.18	0.72			

the kinematics, using the energy and angular information. The determination of the center-of-mass angle of the events was performed in two different ways, depending on the exit angles of the particles. The good angular resolution of the detection setup was directly used when one of the two particles was detected in the small laboratory angles (i.e., for the small and large center-of-mass angles). When both particles were detected at large angles, where the angular resolution of the setup was poorer, the center-of-mass angle was calculated from the deposited energies; this case corresponds to intermediate center-of-mass angles. In the first case the angular bins were thus determined by the detector angular resolution; in the second case the events were grouped in bins slightly larger than the uncertainty on the calculated angle. The detection efficiency for the events of interest at each center-of-mass angle was estimated from a simulation of the set-up, based on its geometry and including energy loss effects.

Combining the above information, the ^{4}He(^{6}He, ^{6}He) ^{4}He cross-section values were calculated. The results are listed in Table I, and shown in Fig. 1 as full dots (the curves are results of a fit as explained in the following section). For comparison, the cross-section values previously measured using a gas target are plotted as open dots. The agreement of the two sets of data in the overlapping region is excellent and does not require any scaling. The number of events collected in the three angular regions was about 2000 for the small center-of-mass angles, 950 around 100° and 600 events at angles larger than 150°. The error bars shown in the figure include the statistical errors and the uncertainty related to the determination of the detection efficiency; the latter becomes important at large center-of-mass angles where the role of some parameters (position of the detectors, detection thresholds) is more critical. Overall systematic uncertainties come from the values of the target thickness (~7%) and total beam dose (~5%).

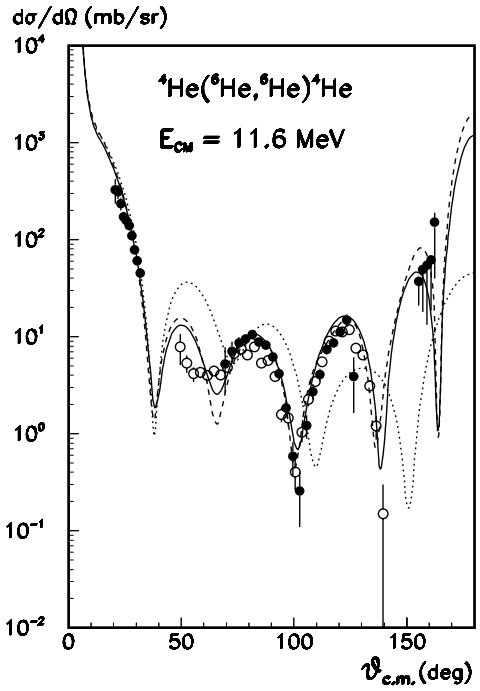

FIG. 1. ^{4}He(^{6}He, ^{6}He)^{4}He cross section at $E_{\text{c.m.}}=11.6$ MeV, measured using a gas target (open dots) and obtained in the present measurement using the ^{4}He-implanted Al target (full dots). The gas-target data are those from Ref. [22], plotted with a finer binning as justified by an evaluation of the angular uncertainties. Results of the fit using the double-folding potential plus a parity-dependent term on the two sets of data are represented by the solid and dashed curves respectively; the dotted curve is the fit without the parity-dependent term.

III. RESULTS AND DISCUSSION

In our previous work [22] the available data were first analyzed in terms of an optical-model potential (OM), and then with a double-folding potential based on a microscopic model for the structure of ^{6}He. Here we review those results in the light of the new data, and perform further comparisons with different calculations.

The best agreement with the previous data was obtained using the double-folding potential V_{DF} [31], with the addition of a parity-dependent term V_{P}; the latter is used to account for the possible elastic transfer process of the two weakly bound neutrons in ^{6}He projectile to the ^{4}He target. The parity-dependent term was essential for the fit, indicating that the previous data already contained evidence of the two-neutron transfer process. The fit on the previous data is represented by the solid curve in Fig. 1. The main effect of V_{P}, with respect to a fit where the term was not included (dotted curve in Fig. 1), was to produce a sizable increase of the cross section at large angles. Indeed, the new data points confirm this prediction, as the cross section beyond 150°

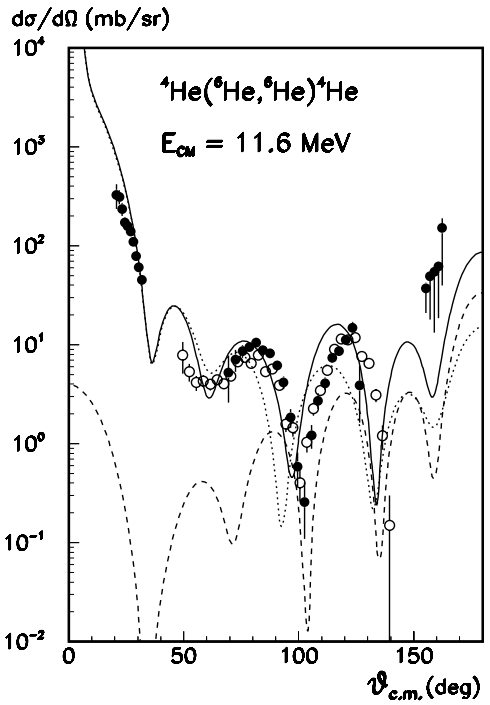

FIG. 2. Results of the DWBA analysis: dotted line, OM fit of the direct elastic scattering; dashed line, DWBA transfer cross section; solid line, coherent addition of the two amplitudes.

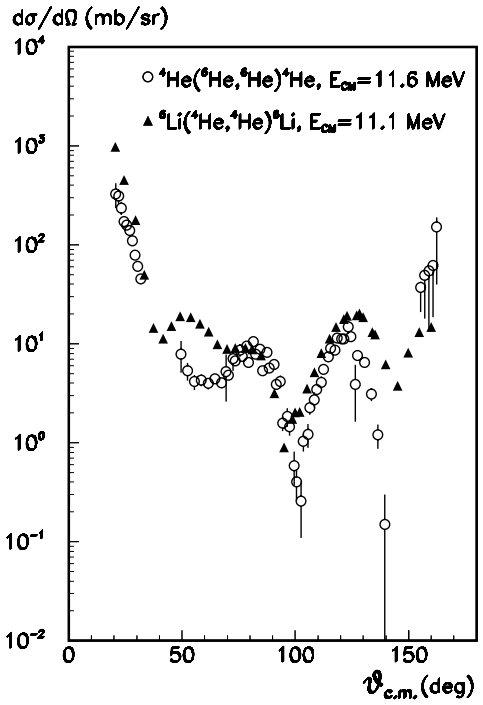

FIG. 3. ^{6}He+^{4}He elastic scattering at $E_{\mathrm{c.m.}}=11.6$ MeV (circles) compared with ^{6}Li+ ^{4}He at $E_{\mathrm{c.m.}}=11.1$ MeV (triangles, from [32]).

rises to about 100 mb/sr. A new fit performed on the whole set (dashed curve in Fig. 1) differs only very slightly from the previous one, and also at small angles the new data points are well reproduced. The conclusion from the analysis with the double folding potential, that the two-neutron transfer process is present in the ^{4}He(^{6}He, ^{6}He)^{4}He elastic scattering at this energy, is confirmed by the new data.

The transfer process was further investigated by means of a distorted-wave Born approximation analysis (DWBA). The points at small angles are important to help choosing the OM parameters for elastic scattering. A reasonable agreement is achieved by using as starting set the parameters from the ^{6}Li(^{4}He, ^{4}He) ^{6}Li scattering at $E_{\mathrm{c.m.}}=11.1$ MeV obtained by Bingham *et al.* [32]. It is important to notice that this is not the only set of parameters, resulting from the analysis in Ref. [32]. The resulting cross section, shown by the dotted curve in Fig. 2, was calculated with the following values of a Woods-Saxon potential with a volume absorption term: $V=191.4$ MeV, $R_{\mathrm{V}}=3.72$ fm, $a_{\mathrm{V}}=0.41$ fm, $W=15.7$ MeV, $R_{\mathrm{W}}=3.96$ fm, $a_{\mathrm{W}}=0.51$ fm. The curve differs from the experimental points at angles larger than 90°. For the calculation of the DWBA transfer amplitude we used a simple model for the ^{6}He nucleus, in which the two weakly bound neutrons are treated as a cluster in a $2s$-state. The cluster wave function was calculated in a Woods-Saxon potential with parameters $R=2.7$ fm, $a=0.7$ fm; the depth was adjusted in order to reproduce the $2n$-binding energy in ^{6}He, $S_{2n}=0.973$ MeV. The DWBA amplitude alone is indicated by the dashed curve in Fig. 2; the result of coherent addition of the direct and transfer amplitudes is represented by the solid line. The agreement, though not optimal, is improved at larger angles, where the transfer amplitude accounts for the increase of the experimental cross section. It is interesting to notice how the contribution of the transfer process is sizable in a very wide angular range; interference with the direct elastic scattering is important already around 60°–70°. At this low center-of-mass energy the situation is very different from the same ^{4}He(^{6}He, ^{6}He) ^{4}He reaction at $E_{\mathrm{c.m.}}=60.4$ MeV measured at the Flerov Laboratory in Dubna [21]. At the higher energy the two contributions are well separated as function of the angle and the transfer process can be studied in detail [33,34]. In the present conditions, there are ambiguities due to the interference and the uncertainties on the OM parameters; also, the importance of a sequential transfer process, not included in the analysis, cannot be ruled out at this low energy. This suggests that the DWBA analysis may not be the most indicated for the investigation of the way in which the fine details of the structure of ^{6}He play a role in the transfer process.

In Fig. 3 our data are compared with the experimental points from the ^{6}Li+ ^{4}He scattering of Ref. [32]. Given the resemblance between the ^{6}He and ^{6}Li nuclei—both have a large matter radius, and have pronounced cluster structures—the two reactions are expected to be rather similar. The cross sections show that this is in fact the case, still there are significant differences at angles between 40° and 70°, and at large angles where the oscillations in the ^{6}He+ ^{4}He case are more pronounced. The quality of the experimental points should allow to single out the differences between the structure of the ^{6}He and ^{6}Li systems, in particular the importance of the different clustering modes. However, a more complete description of the reaction is necessary, possibly including an explicit treatment of the channels that may be coupled to the elastic scattering.

Recently, other studies of the ^{4}He(^{6}He, ^{6}He)^{4}He reaction have been presented, which try to describe the complexity of the reaction mechanism. The resonating-group method (RGM) has been applied in Refs. [35] and [36]. The RGM is a microscopic treatment, which is parameter-free once the nucleon-nucleon interaction is chosen; also, since the total scattering wave function is properly antisymmetrized, the effect of the elastic transfer process is taken into account. However, a direct comparison of these calculations with our data is difficult. In Ref. [35] the relevant results concern an energy range somewhat lower. In Ref. [36] the authors focus on the ^{8}He+α scattering, and include only a comparison with the ^{6}He+α case, which is calculated by using a much simplified model for the structure of ^{6}He.

The importance of the breakup channels in reactions involving weakly bound and halo nuclei has been recently underlined in several occasions [37–39]. In the ^{6}He+^{4}He case considered here, they may play an important role, and in particular they may help explaining the differences compared to the ^{6}Li+^{4}He case as the breakup threshold is in the first case lower. A first attempt for such a description has been already performed by Rusek *et al.* [40,41], with continuum-discretized coupled-channel calculations (CDCC) of the two reactions; however, the authors use simplified two-cluster models for the description of ^{6}He (as $\alpha+2n$) and ^{6}Li (as $\alpha+d$). Concerning the present data, they report that the inclusion of the transfer process in the ^{6}He + ^{4}He reaction at $E_{\mathrm{c.m.}}=11.6$ MeV does not lead to a satisfactory agreement with the data. In another analysis, the coupled reaction channels method (CRC) has been applied to the ^{6}He+^{4}He reaction at $E_{\mathrm{c.m.}}=60.4$ MeV [42]. The 2n-transfer has been treated in a microscopic approach, including different one-step and two-step processes proceeding via the 2^+ excited state in ^{6}He, and sequential transfer. The results are very encouraging, and a similar study on the low-energy data presented here is in preparation [43].

IV. CONCLUSIONS

We have measured the ^{4}He(^{6}He, ^{6}He) ^{4}He elastic cross section at $E_{\mathrm{c.m.}}=11.6$ MeV by using a ^{4}He-implanted Al foil as target, which allowed to enlarge the angular range in which data were collected with respect to a previous measurement. The values of the cross section are measured with good precision between 20° and 160° in the center of mass; at backward angles, the new data show an increase of the cross section. Comparison with different calculations show that this rise cannot be explained by using a potential describing the elastic scattering only: both the OM potential, and a more sophisticated double-folding potential based on a microscopic model for ^{6}He fail in this respect. In order to reproduce the experimental data, it is necessary to include a term that accounts for the 2n-transfer: this was shown by using a parity-dependent term, or a DWBA transfer amplitude. While this confirms the presence of the transfer process in the experimental data, the extraction of further information on ^{6}He is hindered by the complexity of the process at this energy, and the uncertain role of other mechanisms, such as the breakup, which couple to the elastic scattering. Other recent analyses have been reviewed, which take into account the transfer in a natural way (the RGM analysis), or consider the role of the breakup channels (the CDCC calculations); these contain still several approximations, and do not reach a satisfactory agreement with the experimental data. The comparison of the ^{6}He+^{4}He elastic cross section with the ^{6}Li +^{4}He one at similar energy show how the quality of the data may allow to identify the differences between the two systems.

ACKNOWLEDGMENTS

The authors would like to thank the staff of the Cyclotron Research Center in Louvain-la-Neuve for their dedication to the production of the ^{6}He beam and their assistance during these measurements. We also thank Dr R. Wolski and Dr K. Rusek for useful discussions. This work presents results of research funded by the Belgian Program on Interuniversity Poles of Attraction (P.A.I./I.U.A.P., P4/18) initiated by the Belgian Federal Services of Scientific, Technical, and Cultural Affairs. This work is also supported by the Flemish Funds for Scientific Research (F.W.O. Vlaanderen).

[1] I. Tanihata *et al.*, Phys. Lett. B **160**, 380 (1985).
[2] I. Tanihata, H. Hamagaki, O. Hashimoto, Y. Shida, N. Yoshikawa, K. Sugimoto, O. Yamakawa, T. Kobayashi, and N. Takahashi, Phys. Rev. Lett. **55**, 2676 (1985).
[3] P.G. Hansen and B. Jonson, Europhys. Lett. **4**, 409 (1987).
[4] T. Kobayashi, O. Yamakawa, K. Omata, K. Sugimoto, T. Shimoda, N. Takahashi, and I. Tanihata, Phys. Rev. Lett. **60**, 2599 (1988).
[5] N.A. Orr *et al.*, Phys. Rev. Lett. **69**, 2050 (1992).
[6] A.A. Korsheninnikov and T. Kobayashi, Nucl. Phys. A **567**, 97 (1994).
[7] T. Aumann, L.V. Chulkov, V.N. Pribora, and M.H. Smedberg, Nucl. Phys. A **640**, 24 (1998).
[8] M. Zinser *et al.*, Nucl. Phys. A **619**, 151 (1997).
[9] T. Aumann *et al.*, Phys. Rev. C **59**, 1252 (1999).
[10] M.J.G. Borge *et al.*, Z. Phys. A **340**, 255 (1991).
[11] V.I. Kukulin, V.M. Krasnopolsky, V.T. Voronchev, and P.B. Sazonov, Nucl. Phys. A **453**, 365 (1986).
[12] M.V. Zhukov, B.V. Danilin, D.V. Fedorov, J.M. Bang, I.J. Thompson, and J.S. Vaagen, Phys. Rep. **231**, 151 (1993).
[13] J. Wurzer and H.M. Hofmann, Phys. Rev. C **55**, 688 (1997).
[14] A. Yoshida *et al.*, Phys. Lett. B **389**, 457 (1996).
[15] P.A. DeYoung *et al.*, Phys. Rev. C **58**, 3442 (1998).
[16] J.J. Kolata *et al.*, Phys. Rev. Lett. **81**, 4580 (1998).
[17] C. Signorini *et al.*, Eur. Phys. J. A **2**, 227 (1998).
[18] M. Trotta *et al.*, Phys. Rev. Lett. **84**, 2342 (2000).
[19] L.V. Chulkov *et al.*, Phys. Rev. Lett. **79**, 201 (1997).
[20] D. Aleksandrov *et al.*, Nucl. Phys. A **633**, 234 (1998).
[21] G.M. Ter-Akopian *et al.*, Phys. Lett. B **426**, 251 (1998).
[22] R. Raabe *et al.*, Phys. Lett. B **458**, 1 (1999).

[23] R. Wolski *et al.*, Phys. Lett. B **467**, 8 (1999).
[24] A.N. Ostrowski, A.C. Shotter, S. Cherubini, T. Davinson, D. Groombridge, A.M. Laird, A. Musumarra, A. Ninane, M.-G. Pellegritti, and A. di Pietro, Phys. Rev. C **63**, 024605 (2001).
[25] W. von Oertzen and H.G. Bohlen, Phys. Rep. **19**, 1 (1975).
[26] G. Ryckewaert, J.M. Colson, M. Gaelens, M. Loiselet, and N. Postiau, Nucl. Phys. A **701**, 323c (2002).
[27] G. Demortier, Nucl. Instrum. Methods Phys. Res. B **66**, 51 (1992).
[28] L. Weissman, R. Raabe, M. Huyse, G. Koops, H. Pattyn, G. Terwagne, and P. Van Duppen, Nucl. Instrum. Methods Phys. Res. B **170**, 266 (2000).
[29] R. Raabe *et al.*, Nucl. Phys. A **701**, 387c (2002).
[30] T. Davinson *et al.*, Nucl. Instrum. Methods Phys. Res. B **454**, 350 (2000).
[31] D. Baye, L. Desorgher, D. Guillain, and D. Herschkowitz, Phys. Rev. C **54**, 2563 (1996).
[32] H.G. Bingham, K.W. Kemper, and N.R. Fletcher, Nucl. Phys. A **175**, 374 (1971).
[33] Y.T. Oganessian, V.I. Zagrebaev, and J.S. Vaagen, Phys. Rev. Lett. **82**, 4996 (1999).
[34] Y.T. Oganessian, V.I. Zagrebaev, and J.S. Vaagen, Phys. Rev. C **60**, 044605 (1999).
[35] K. Fujimura, D. Baye, P. Descouvemont, Y. Suzuki, and K. Varga, Phys. Rev. C **59**, 817 (1999).
[36] D. Baye, P. Descouvemont, and R. Kamouni, Few-Body Syst. **29**, 131 (2000).
[37] N.K. Timofeyuk and R.C. Johnson, Phys. Rev. C **59**, 1545 (1999).
[38] C. Signorini *et al.*, Phys. Rev. C **61**, 061603(R) (2000).
[39] A. Bonaccorso and F. Carstoiu, Nucl. Phys. A **706**, 322 (2002).
[40] K. Rusek, P.V. Green, P.L. Kerr, and K.W. Kemper, Phys. Rev. C **56**, 1895 (1997).
[41] K. Rusek and K.W. Kemper, Phys. Rev. C **61**, 034608 (2000).
[42] I.V. Krouglov, M. Avrigeanu, and W. von Oertzen, Eur. Phys. J. A **12**, 399 (2001).
[43] W. von Oertzen (private communication).